

Approximating Optimal State Estimation

Brian F. Farrell
Harvard University

Petros J. Ioannou
University of Athens

Seminar on Recent Developments in
Atmospheric and Ocean Data Assimilation, ECMWF
Thursday, Sept. 11, 2003

Motivation for optimal state estimation

- Approximate two day error doubling times imply that reducing analysis error could significantly increase forecast accuracy.
- Presently assimilation systems have errors approximately equal to observational errors suggesting that the analysis is suboptimal.
- Improving the analysis is most effectively accomplished by implementing approximate optimal state estimation which utilizes the model to make the best use of observational resources.

Implementing optimal state estimation

- The high dimension of the error system is an obstacle because forecast error structure information is crucial to implementing optimal observer strategies.
- But in fact the dimension of the dynamically relevant error system is manageably small.
- Problem is to obtain a reduced order error system and exploit it to implement approximate optimal state estimation.
- Our approach to this problem uses balanced truncation to optimally reduce the error system dimension and construct a reduced order Kalman filter.
- Practical implementation of this optimal observation strategy exploits the restricted formal equivalence of the Kalman filter and 4D-Var to make use of existing operational forecast resources.

Optimally reducing forecast error system order

- Minimal dimension forecast error system must take account of error system dynamics in a way that grid point or harmonic functions bases which are not problem specific can not.
- Examples of problem adaptive bases are the eigenmodes of the system operator and the EOF's identified by stochastically forcing the system (POD).
- But the eigenmodes and EOF's are generally not an optimal basis for the dynamics.
- Both the EOF's and SO's must be retained in an optimally truncated basis for the dynamics.

- The preferred response structures are obtained from the covariance matrix:

$$\mathbf{P} = \int_0^{\infty} e^{\mathbf{A}t} e^{\mathbf{A}^\dagger t} dt ,$$

which satisfies the Lyapunov equation:

$$\mathbf{A} \mathbf{P} + \mathbf{P} \mathbf{A}^\dagger = -\mathbf{I} .$$

The eigenvectors of \mathbf{P} are the EOF's.

- The preferred excitation structures are obtained from the stochastic optimal matrix:

$$\mathbf{Q} = \int_0^{\infty} e^{\mathbf{A}^\dagger t} e^{\mathbf{A}t} dt ,$$

which satisfies the back Lyapunov equation:

$$\mathbf{A}^\dagger \mathbf{Q} + \mathbf{Q} \mathbf{A} = -\mathbf{I} .$$

The eigenvectors of \mathbf{Q} are the SO's.

- i) For non-normal systems: EOFs \neq SO's
- ii) Both EOF's and SO's must be retained in order to accurately represent the dynamics.
- iii) If the system is normal the SO's and the EOF's coincide (they are identical to the eigenmodes of the system) and in that case a k order truncation corresponds to retaining the k least damped modes of the system.
- (iv) This modal truncation is not optimal for non-normal systems in which the SO's, EOF's and modes are not the same.
- (v) If there were a coordinate system in which the EOF's and the SO's become the same, then in that coordinate system we could proceed with modal truncation as in normal systems. Such a transformation exists and this procedure is called balancing and the coordinates in which both the P and Q are transformed to a diagonal matrix Σ is called the balanced realization (Moore, 1981; Zhou and Doyle, 1998).

Truncation of the dynamics

Consider the N order dynamical system:

$$\frac{d\psi}{dt} = \mathbf{A}\psi$$

We seek a k order truncation of this N dimensional system:

$$\frac{d\psi_k}{dt} = \mathbf{A}_k\psi_k$$

where \mathbf{A}_k is the reduced $k \times k$ dynamical matrix, with $k < N$. This is accomplished by the transformation:

$$\tilde{\psi} = \mathbf{X}\psi_k \quad , \quad \psi_k = \mathbf{Y}^\dagger \tilde{\psi}$$

$$\mathbf{Y}^\dagger \mathbf{X} = \mathbf{I}_k$$

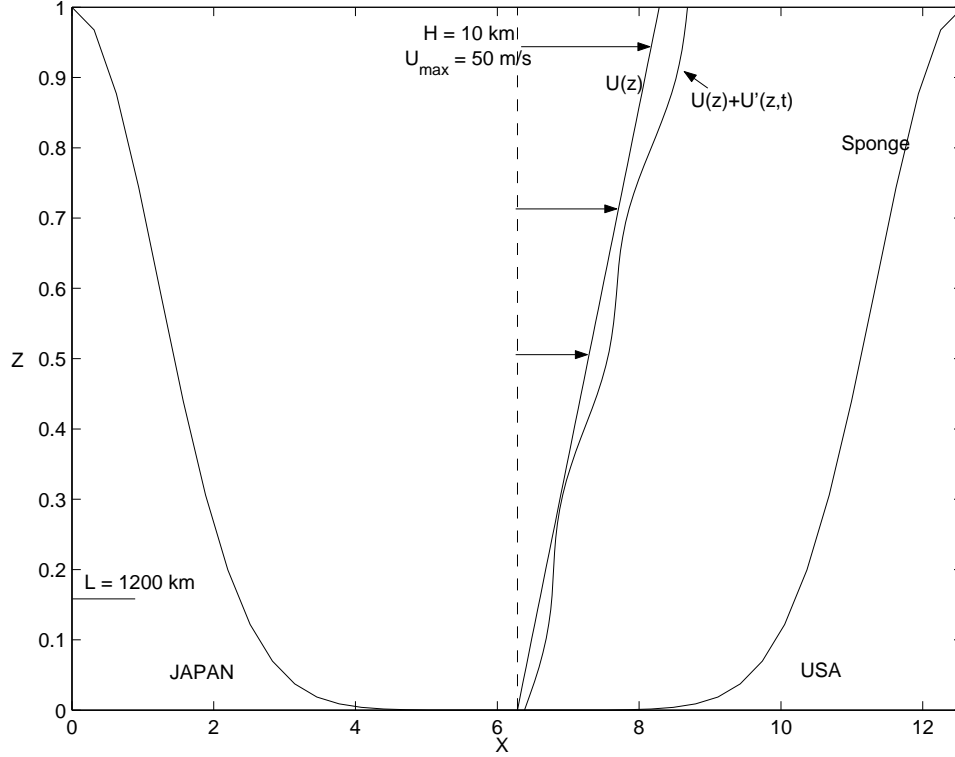
with transformed operator:

$$\mathbf{A}_k = \mathbf{Y}^\dagger \mathbf{A} \mathbf{X}$$

in which \mathbf{X} and \mathbf{Y} simultaneously diagonalize \mathbf{P} and \mathbf{Q} . In transformed coordinates:

$$\mathbf{P}_k = \mathbf{Y}^\dagger \mathbf{P} \mathbf{Y} \quad , \quad \mathbf{Q}_k = \mathbf{X}^\dagger \mathbf{Q} \mathbf{X} \quad .$$

A storm track model example



$$\frac{\partial \phi}{\partial t} = \nabla^{-2} \left[-U(z) \nabla^2 D_x \phi - \left(\beta - \frac{d^2 U(z)}{dz^2} \right) D_x \phi - r(x) \nabla^2 \phi \right]$$

$$\frac{\partial^2 \phi}{\partial t \partial z} = -U(0) D_x \frac{\partial \phi}{\partial z} + U'(0) D_x \phi - r(x) \frac{\partial \phi}{\partial z} - \Gamma_g (D_x^2 - l^2) \phi \quad \text{at } z = 0$$

$$\frac{\partial^2 \phi}{\partial t \partial z} = -U(1) D_x \frac{\partial \phi}{\partial z} + U'(1) D_x \phi - r(x) \frac{\partial \phi}{\partial z} \quad \text{at } z = 1$$

$$U = U_g + z, \quad \Gamma_g \equiv \frac{N}{U_0} \sqrt{\frac{\nu}{2f}}$$

The mean model storm track perturbation dynamics is governed by:

$$\frac{d\psi}{dt} = \mathbf{A}\psi$$

$$\mathbf{A} = \nabla^{-2} \left(- (U_g + z) D_x \nabla^2 - \beta D_x - r(x) \nabla^2 \right)$$

Discretize with 40 zonal harmonics and 10 levels in the vertical. Total degrees of freedom: $N = 400$

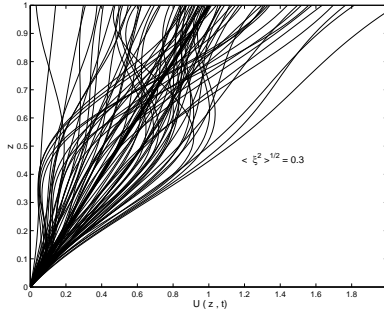


Figure 1: Zonal flow realization of the time dependent storm track model.

For reference the time dependent tangent linear storm track is obtained by considering zonal wind of the form $U_g + z + u(z, t)$. The linear operator becomes $\mathbf{A} + \mathbf{A}_1(t)$ where $\mathbf{A}_1(t)$ is the deviation operator:

$$\mathbf{A}_1(t) = (\nabla^2)^{-1} \left(- u(z, t) D_x \nabla^2 + \frac{d^2 u(z, t)}{dz^2} D_x \right) ,$$

We consider a fluctuating zonal wind of form:

$$u(z, t) = \frac{f_1(t)}{2} [1 - \cos(\pi z/2)] + \frac{f_2(t)}{2} [1 - \cos(2\pi z)] + f_3(t) \sin(\pi z/2) + f_4(t) z^2$$

where $f_i(t)$ is a red noise process with mean zero, standard deviation 0.5, and decorrelation time 1.5 days. The profiles were chosen to give variance increasing with height, and also to lead to almost surely westerly winds. Typical realizations of the resulting mean flow are shown in Fig. 1.

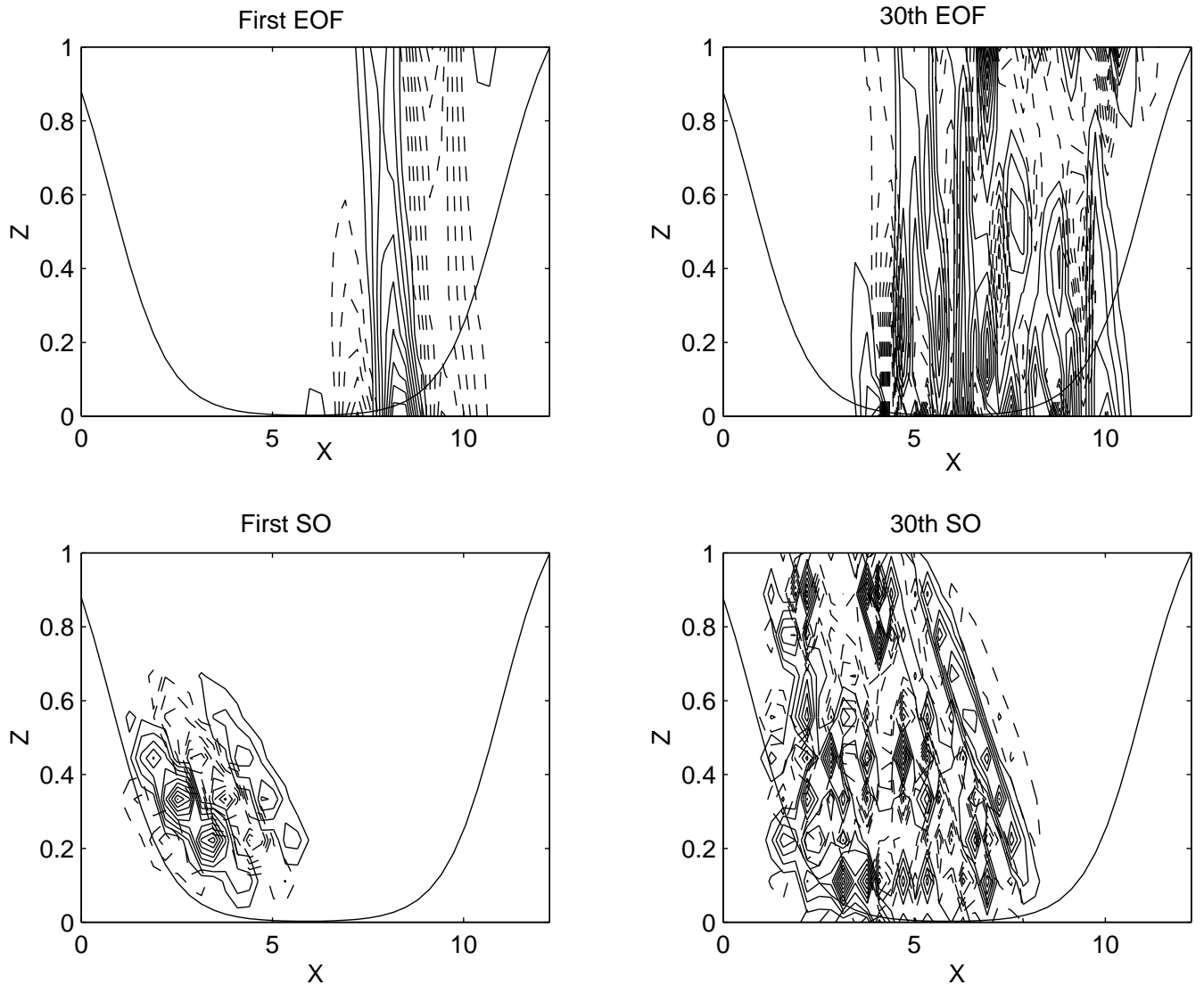


Figure 2: For the stable time mean storm track model. Top panels: The streamfunction of the first and the 30th EOF. The first EOF accounts for 23 % of the maintained variance, the 30th EOF accounts for 0.35 % of the variance. Bottom panels: The structure of the streamfunction of the first and 30th Stochastic Optimal. The first SO is responsible for producing 19.7 % of the maintained variance; the 30th SO is responsible for producing 0.48 % of the maintained variance.

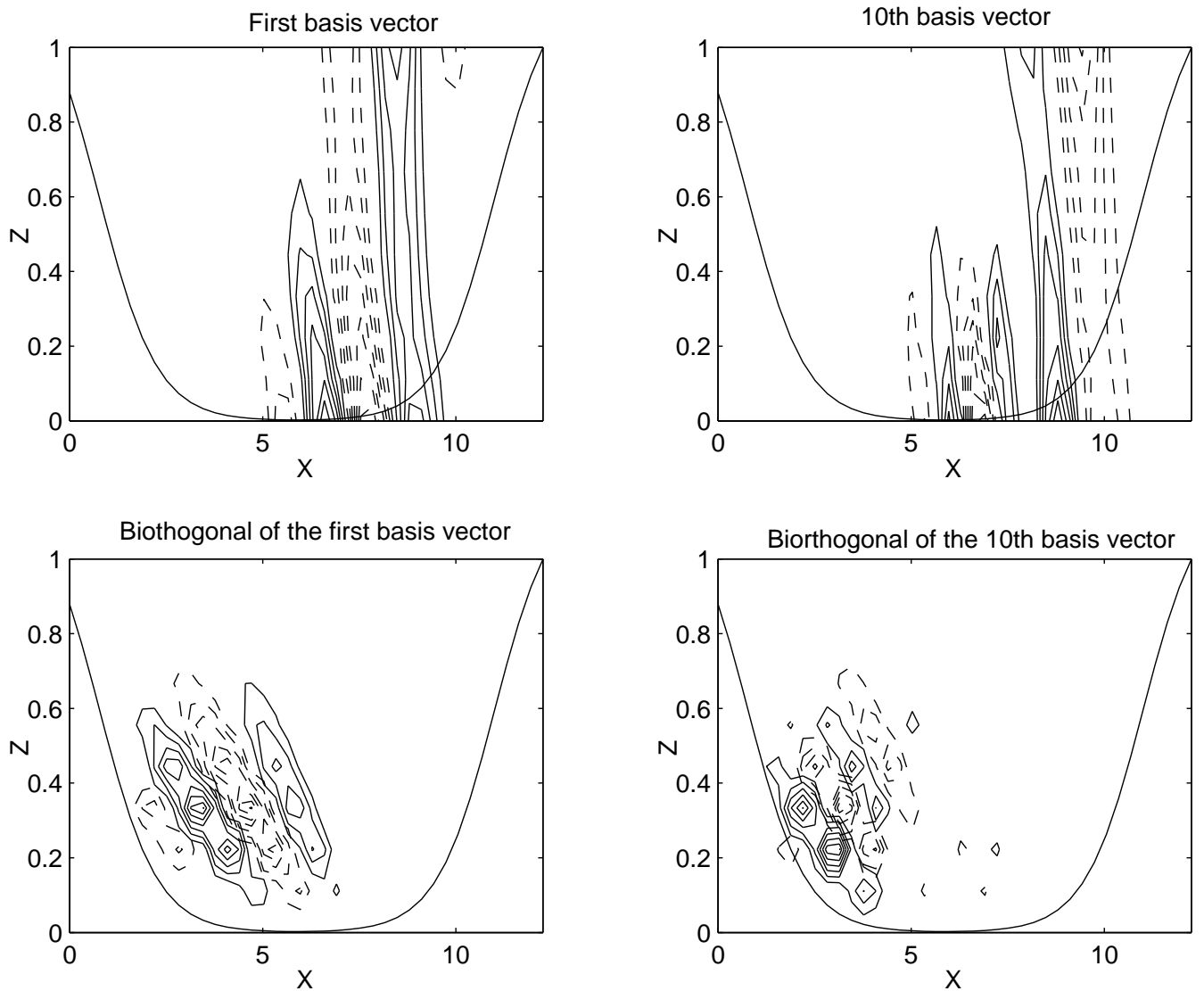


Figure 3: For the stable time mean storm track model. Top left panel: the streamfunction of the first basis vector of the expansion for the balanced truncation of the system. It is given by the first column of \mathbf{X} . Top right panel: the streamfunction of the tenth basis vector of the expansion for the balanced truncation of the system. It is given by the tenth column of \mathbf{X} . Bottom left panel: the streamfunction of the biorthogonal of the first basis vector. It is given by the first column of \mathbf{Y} . Bottom right panel: the streamfunction of the tenth basis vector. It is given by the tenth column of \mathbf{Y} .

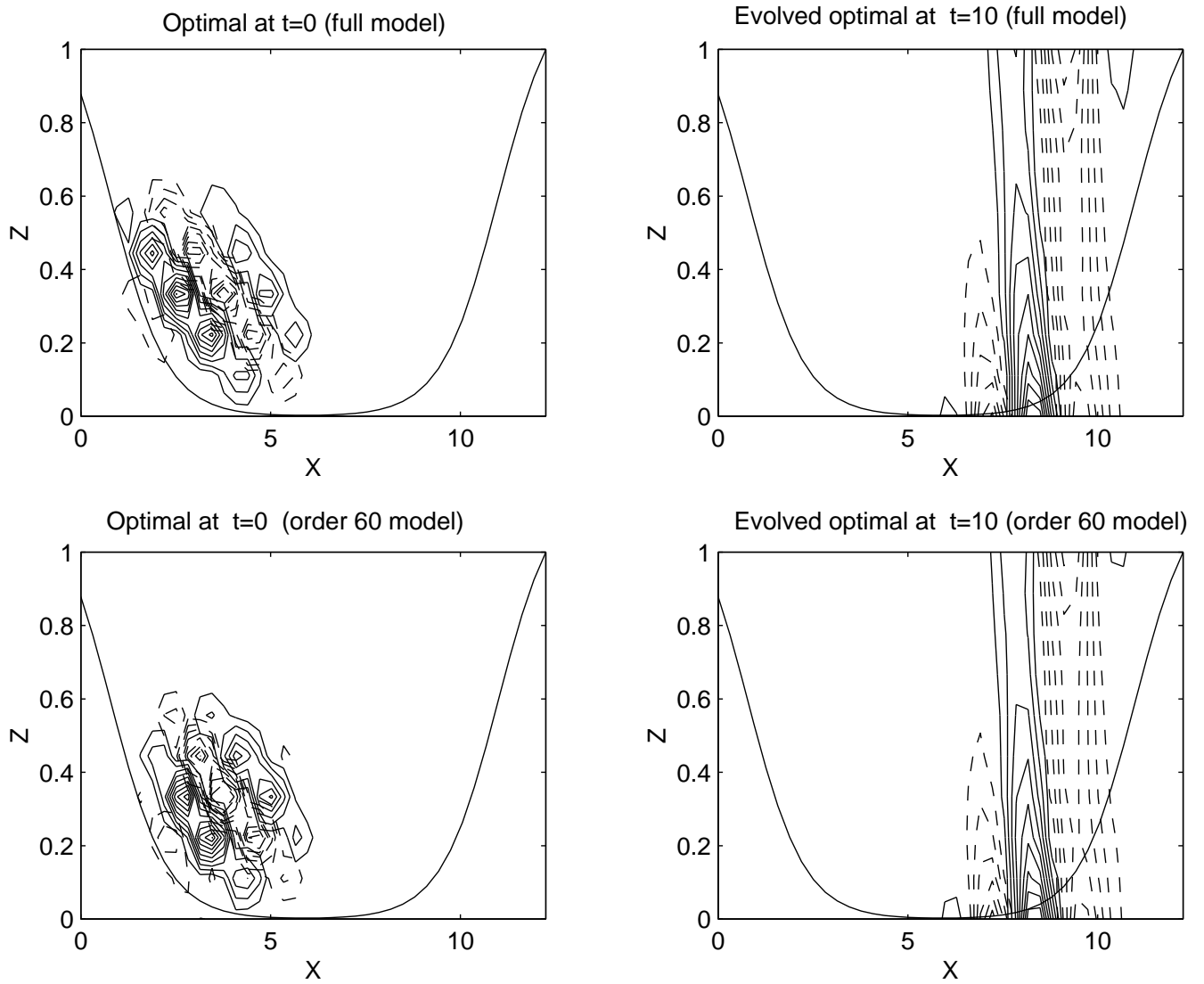


Figure 4: For the stable time mean storm track model. The structure of the streamfunction of the optimal perturbation that leads to the greatest energy growth at $t = 10$ (left panels), and the evolved optimal streamfunction, which is the structure that these optimals evolve into at the optimizing time $t = 10$ (right panels). The top panels are for the full system while the bottom panels are for the order 60 balanced truncation.

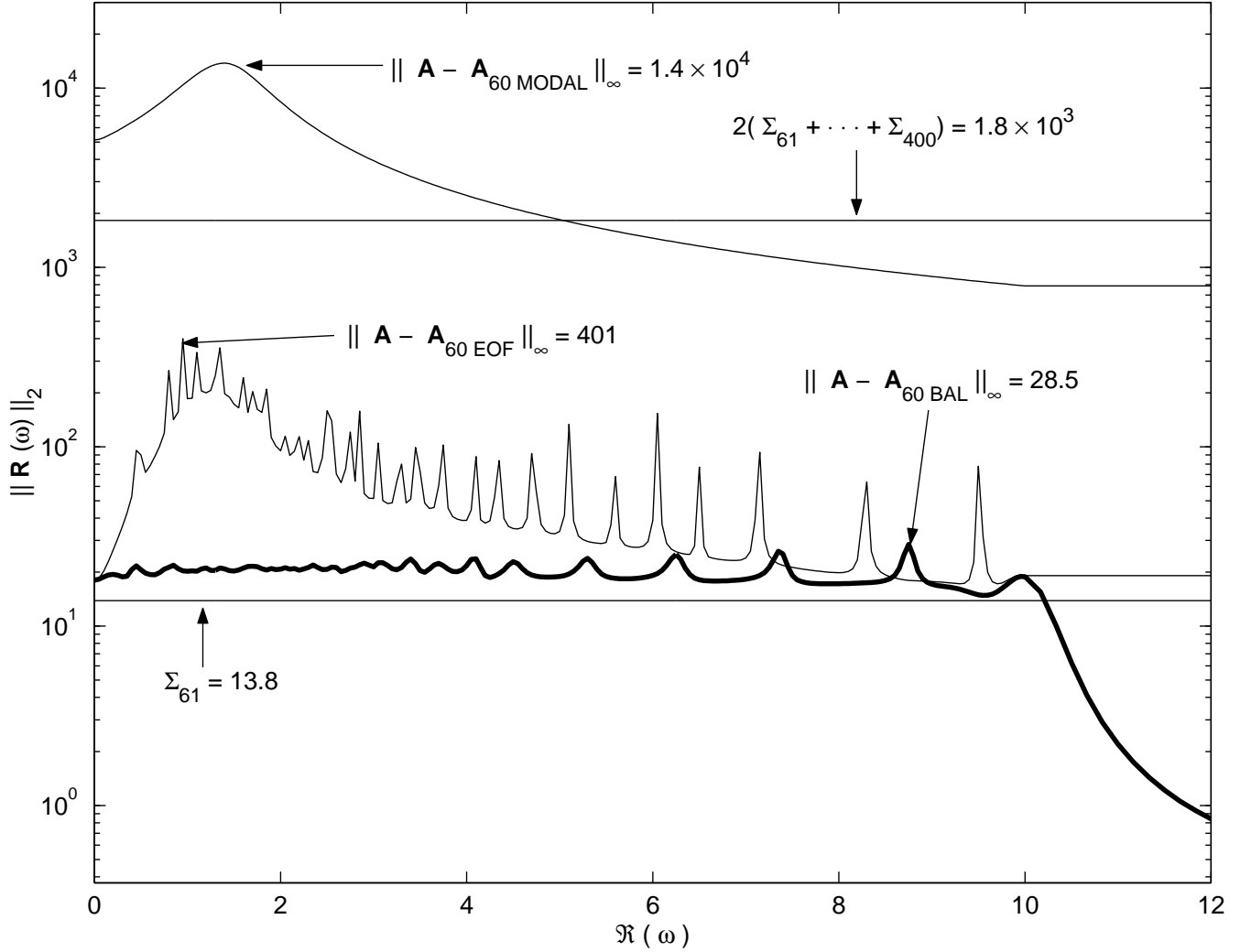


Figure 5: For the stable time mean storm track model: the maximum singular value of the error system $\mathbf{A} - \mathbf{A}_{60}$ as a function of frequency. The system \mathbf{A}_{60} is an order 60 approximation obtained from \mathbf{A} by balanced truncation. The maximum of this curves is the H_∞ error of the order 60 balanced truncation which is found here to be 28.5. Also indicated with a straight line is the theoretical minimum error of an order 60 truncation, which equals the first neglected Hankel singular value $\Sigma_{61} = 13.8$. The balanced truncation is seen to be nearly optimal.

Assimilation as an observer system

Consider assimilating data taken from truth, x_t . The forecast error $e_f = x_f - x_t$ obeys the equation:

$$\frac{de_f}{dt} = \mathbf{A}e_f + \mathbf{Q}^{1/2}w_m ,$$

in which \mathbf{A} is the unstable tangent linear operator and \mathbf{Q} is the model error covariance; w_m is assumed to be a vector of temporally uncorrelated noise processes.

Introduce n observations, y_{ob} . The observations are defined in terms of truth x_t as:

$$y_{ob} = \mathbf{H}x_t + \mathbf{R}^{1/2}w_o$$

where \mathbf{R} is the observational error covariance and w_o is an n vector of white noise processes.

Assimilate these observations to obtain an analysis x_a with analysis error $e_a = x_a - x_t$ satisfying the Luenberger observer system:

$$\begin{aligned} \frac{de_a}{dt} &= \mathbf{A}e_a + \mathbf{K}(y_{ob} - \mathbf{H}x_a) + \mathbf{Q}^{1/2}w_m \\ &= (\mathbf{A} - \mathbf{K}\mathbf{H})e_a + \mathbf{K}\mathbf{R}^{1/2}w_o + \mathbf{Q}^{1/2}w_m . \end{aligned}$$

The gain, \mathbf{K} , is chosen to minimize the analysis error variance $\langle e_a^2 \rangle$.

As generalized stability of the tangent linear forecast system reveals the potential for forecast failures due to initialization error or unresolved forcings, generalized stability analysis of the observer system reveals the forcing structures that lead to failures in the analysis.

The case of an optimal observer

The \mathbf{K} that minimizes the statistically steady analysis error variance $\langle e_a^2 \rangle$ is the Kalman gain.

Let \mathbf{K} be the asymptotic Kalman gain that results from continual assimilation of observations associated with the observation matrix \mathbf{H} . The Kalman gain is:

$$\mathbf{K} = \mathbf{P}\mathbf{H}^\dagger\mathbf{R}^{-1} ,$$

with \mathbf{P} the stabilizing solution of the algebraic Ricatti equation:

$$\mathbf{A}\mathbf{P} + \mathbf{P}\mathbf{A}^\dagger - \mathbf{P}\mathbf{H}^\dagger\mathbf{R}^{-1}\mathbf{H}\mathbf{P} + \mathbf{Q} = 0 .$$

It is a property of the Kalman filter that the matrix \mathbf{P} obtained as a solution of the algebraic Ricatti equation is also the error covariance of the observer system:

$$\frac{de_a}{dt} = (\mathbf{A} - \mathbf{K}\mathbf{H})e_a + \mathbf{K}\mathbf{R}^{1/2}w_o + \mathbf{Q}^{1/2}w_m .$$

In assimilation a sequential form of the filter is used.

The 4D-Var as an observer system

The 4D-Var assimilation is a special case of an observer in which a background error covariance \mathbf{B} is advanced for T units of time. The error covariance is then:

$$\mathbf{P} = e^{\mathbf{A}T} \mathbf{B} e^{\mathbf{A}^\dagger T} ,$$

from which we calculate the gain:

$$\mathbf{K}_{4D-Var} = \mathbf{P} \mathbf{H}^\dagger (\mathbf{H} \mathbf{P} \mathbf{H}^\dagger + \mathbf{R})^{-1} .$$

The error in this time independent version is obtained by calculating the variance

$$(\mathbf{A} - \mathbf{K}_{4D-Var} \mathbf{H}) \mathbf{P} + \mathbf{P} (\mathbf{A} - \mathbf{K}_{4D-Var} \mathbf{H})^\dagger + \mathbf{K}_{4D-Var} \mathbf{R} \mathbf{K}_{4D-Var}^\dagger + \mathbf{Q} = 0 .$$

In assimilation studies 4D-Var is applied sequentially over assimilation intervals of length T .

Reduced order error covariance estimate

The error covariance is advanced in the truncated space to obtain a reduced Kalman gain. The observer system in reduced coordinates is:

$$\frac{de_k}{dt} = (\mathbf{A}_k - \mathbf{K}_k \mathbf{H}_k) e_k + \mathbf{K}_k \mathbf{R}_k^{1/2} w_o - \mathbf{Q}_k^{1/2} w_m .$$

where the reduced analysis is $e_k = \mathbf{Y}^\dagger e_a$ for $k \ll N$ and the reduced $k \times k$ operator is:

$$\mathbf{A}_k = \mathbf{Y}^\dagger \mathbf{A} \mathbf{X}$$

The n observations, y_{ob} , are assimilated in the reduced space according to:

$$y_{ob} = \mathbf{H}_k x_k + \mathbf{R}^{1/2} w_o$$

where the reduced order observation matrix is:

$$\mathbf{H}_k = \mathbf{H} \mathbf{X}$$

The error system in the reduced space is used to obtain the Kalman gain \mathbf{K}_k and propagate the error covariance,

$$\mathbf{P}_k = \langle e_k e_k^T \rangle .$$

The error covariance of the full system is then approximated from the reduced covariance \mathbf{P}_k by:

$$\mathbf{P} = \mathbf{X} \mathbf{P}_k \mathbf{X}^\dagger$$

This error covariance is used in 4D-Var.

Evaluation of optimal state estimation and 4D-Var as a function of the number of observations

In continual data assimilation as the number of observations $n \rightarrow \infty$ the square error $\langle e_a^2 \rangle$ of the Kalman filter in the absence of model error behaves as

$$\langle e_a^2 \rangle \approx \frac{1}{n} ,$$

and in the presence of model error as

$$\langle e_a^2 \rangle \approx \frac{1}{n^{1/2}} .$$

For 4D-Var with model error the error asymptotes to a finite value.

We demonstrate these results in the scalar error system:

$$\frac{de_f}{dt} = ae_f + q^{1/2}w_m ,$$

and in the unstable storm track model with the background B for 4D-Var taken to be the identity matrix.

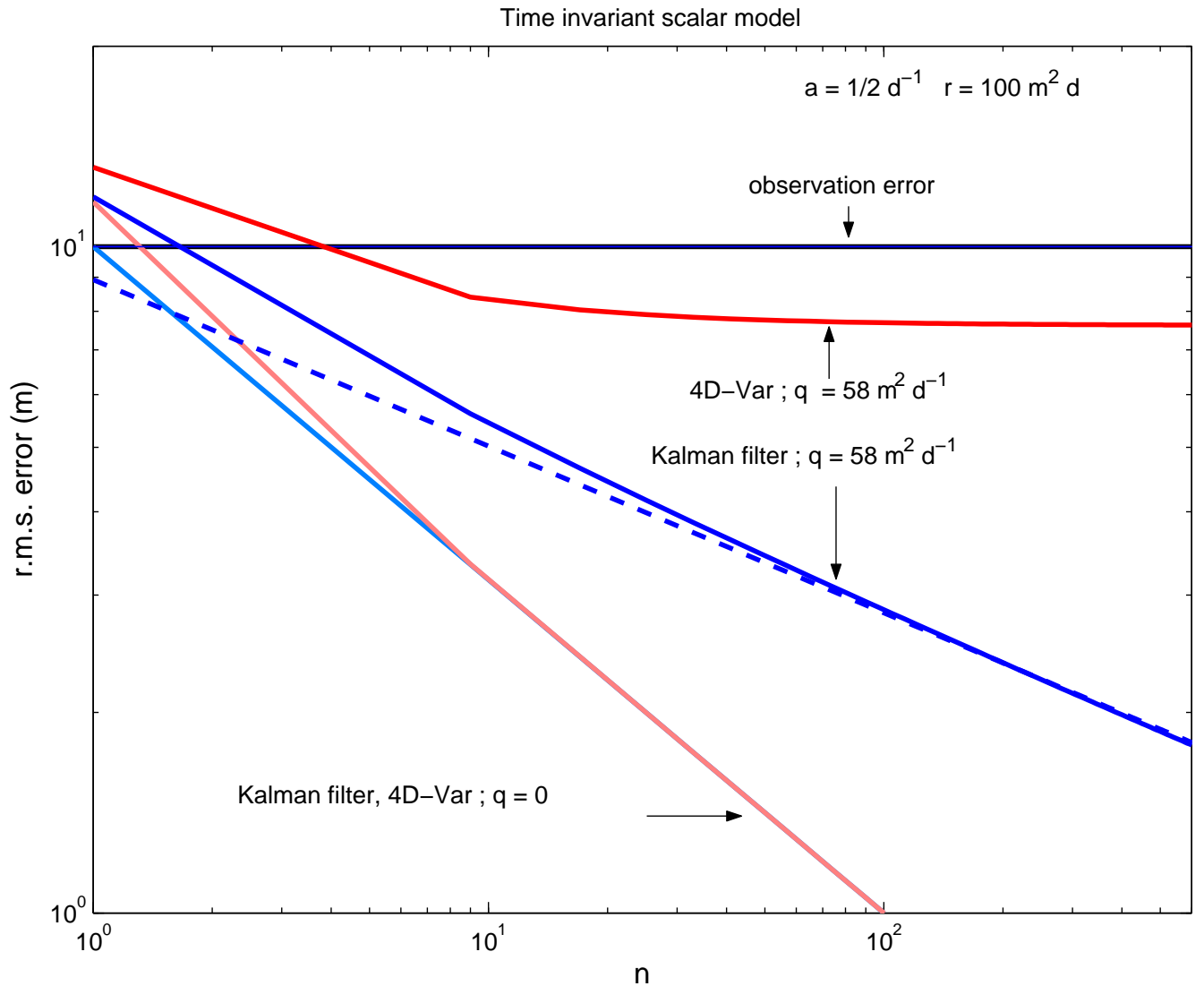


Figure 6: Error in the scalar optimal observer system and a scalar system with an equivalent 4D-Var observer as a function of the number of observations. The gain in the optimal observer is the asymptotic Kalman gain. The growth rate is $a = 1/2 \text{ d}^{-1}$, the observational error is 10 m . The model error variance is $q = 58 \text{ m}^2 \text{ d}^{-1}$ resulting in a model induced error of 10 m after a day. With $q = 0$ the error in both the observer system with the Kalman filter and the 4D-Var falls as $n^{-1/2}$. With $q \neq 0$ the error in the 4D-Var observer asymptotes to a constant value while in the observer with the Kalman filter falls as $n^{-1/4}$.

Error as a function of the number of observation in the time mean storm track model

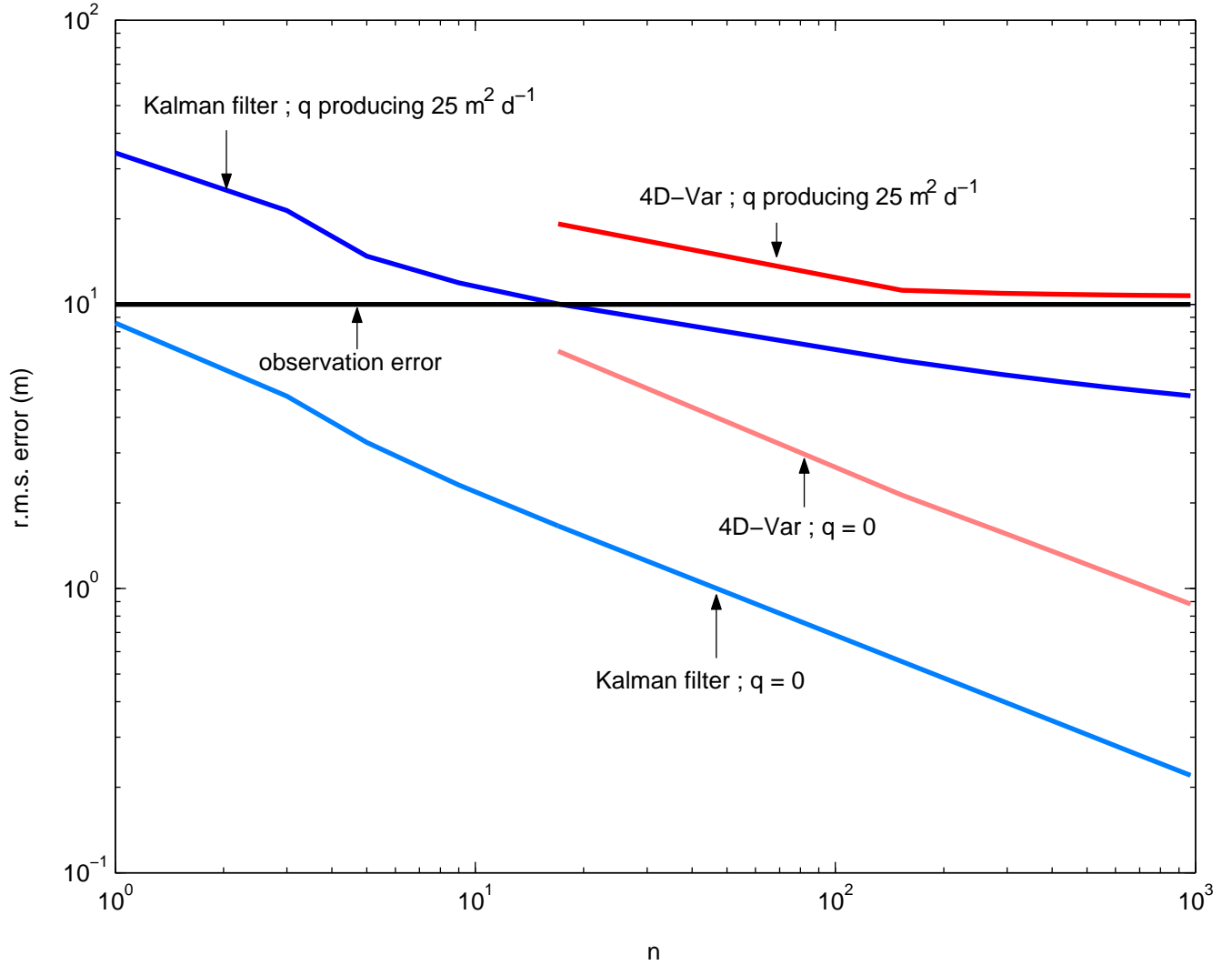


Figure 7: Storm track model error for the optimal observer system and for an equivalent 4D-Var system as a function of the number of observations. The gain in the optimal observer is the asymptotic Kalman gain. The observational error variance is $r = 100 \text{ m}^2 \text{ d}$. The model error is chosen so that an r.m.s. error of 5 m accumulates in a day. With $q = 0$ the error in both the observer system with the Kalman filter and the 4D-Var falls off as $n^{-1/2}$ and eventually becomes identical in both systems. With $q \neq 0$ the error in the 4D-Var observer asymptotes to a constant value while in the observer with the Kalman filter falls off as $n^{-1/4}$ (indicated with the dashed curve). This time mean storm track error model is unstable and 4D-Var requires a number of observations to become stable.

Localization of the Kalman gain by model error

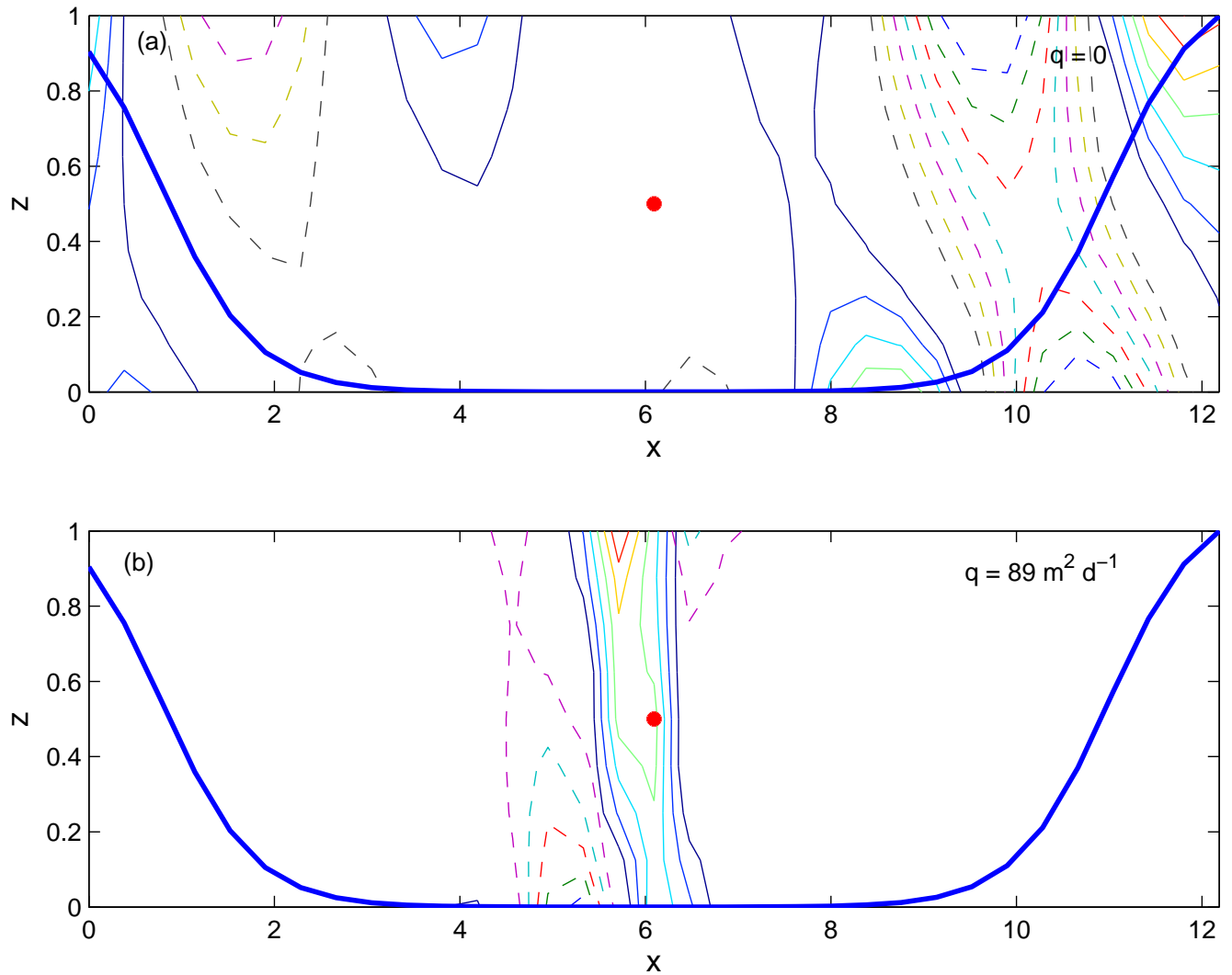


Figure 8: The asymptotic Kalman gain for observation at the center of the channel in the storm track model. Top panel the gain for the case of no model error. Bottom panel the gain for the case with model error. The model error q produces an r.m.s. model error of 5 m in a day. The r.m.s. observational error is 10 m. The asymptotic Kalman gain has been calculated for the time mean flow. Note that the model error leads to localization of the gain in the neighborhood of the observations.

Evolution of the equivalent gain in 4D-Var

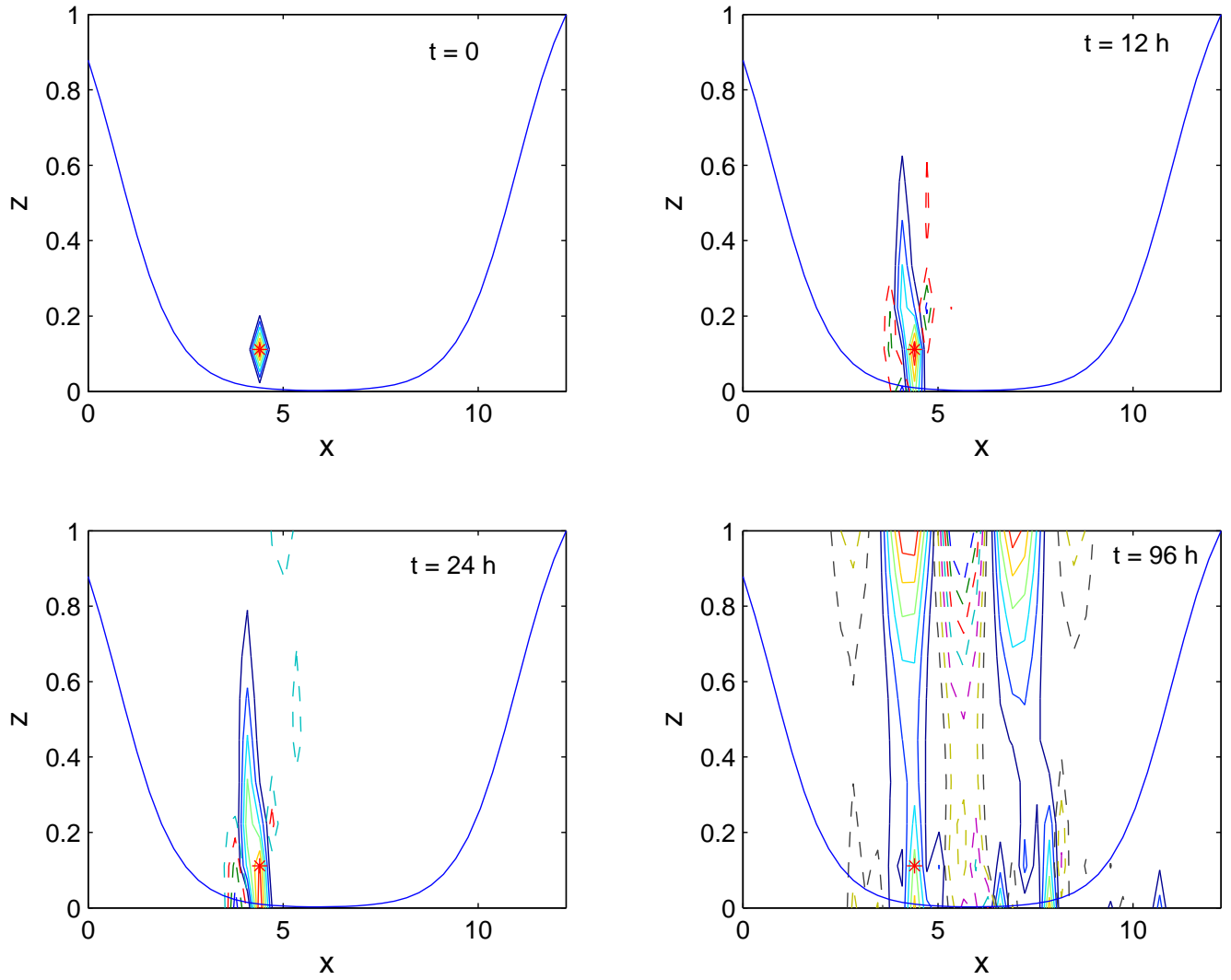


Figure 9: Evolution of the gain associated with the observation marked with a star in 4D-Var as a function of the assimilation interval in the unstable time mean storm track error model. The background \mathbf{B} matrix is the identity. As the assimilation interval increases 4D-Var gains extend into the far field.

**Analysis error in a 4D-Var simulation of the tangent linear storm track model as a function of the assimilation interval.
Perfect model and 16 observations.**

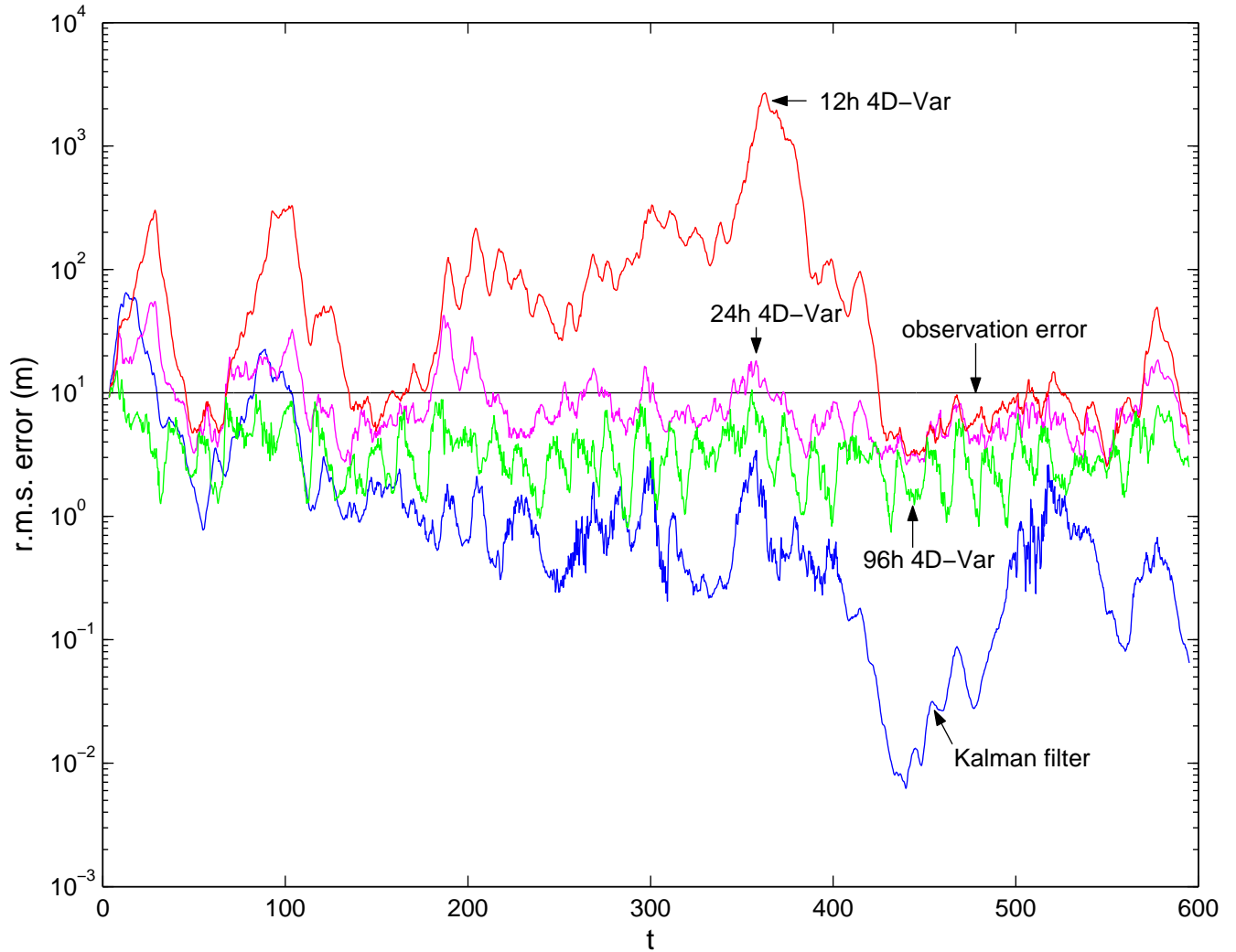


Figure 10: Analysis error of the time dependent storm track model with no model error. The data is assimilated with 4D-Var over the assimilation interval of 12 *h*, 24 *h* and 96 *h*. The background \mathbf{B} is the identity. Also shown is the error obtained with sequential application of a Kalman filter. Under the perfect model assumption 4D-Var becomes equivalent to a Kalman filter as the assimilation interval increases. 16 observations are assimilated with r.m.s. observational error of 10 *m*. Note that assimilation failures are present in all the observer systems, but the excursions are more pronounced in the 12 *h* 4D-Var. The analysis failures can be traced to optimal growth in the observer system.

Approach of 4D-Var to Kalman filter as assimilation interval increases Perfect model and 16 observations

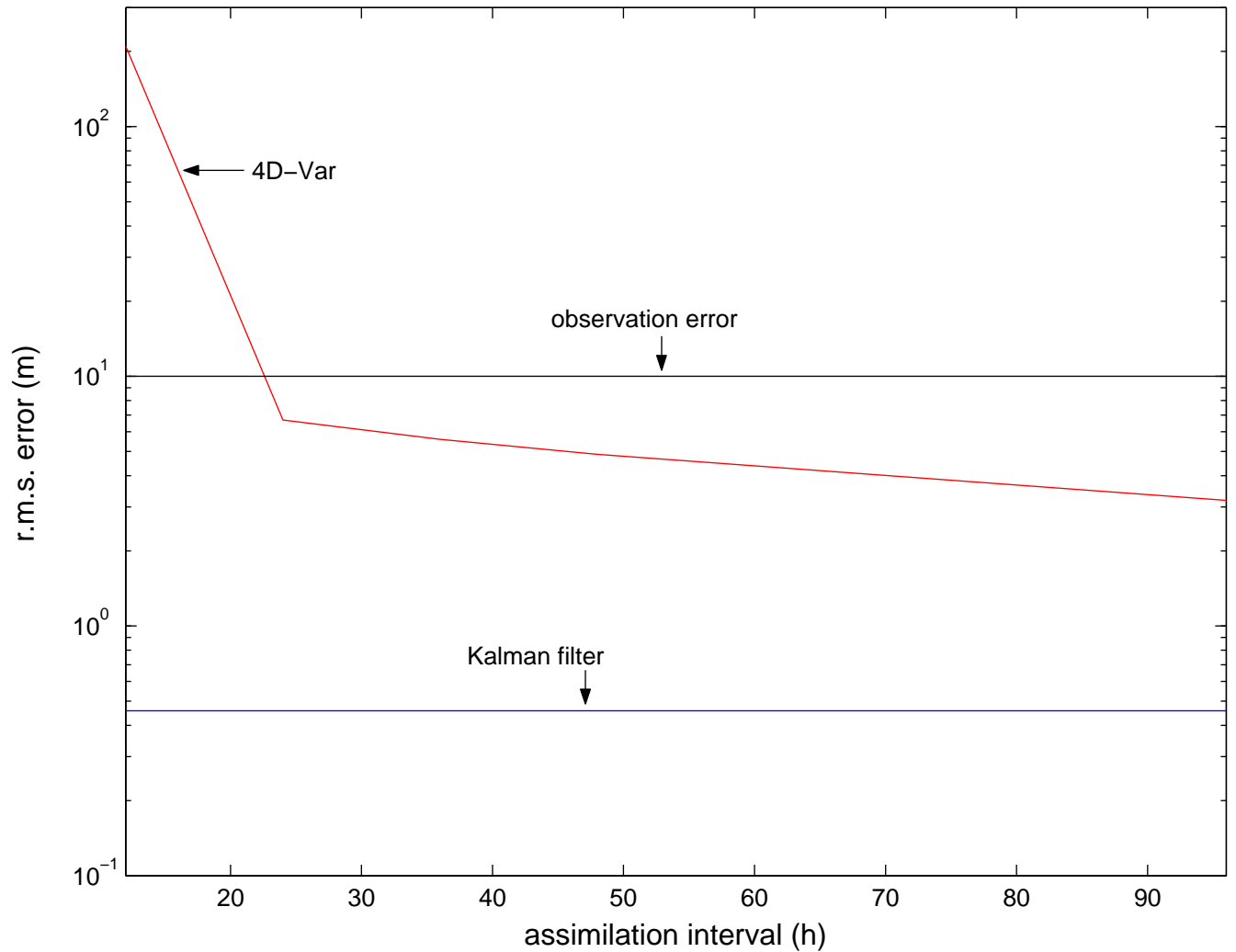


Figure 11: Error in 4D-Var assimilations in the time dependent storm track model with no model error as a function of assimilation interval. Also shown is the error obtained with sequential application of a Kalman filter. 16 observations are assimilated with r.m.s. observational error of 10 m. As the assimilation interval tends to infinity the 4D-Var error approaches that of the Kalman filter.

**Analysis error in a 4D-Var simulation of the tangent linear storm track model as a function of the assimilation interval.
With model error and 16 observations.**

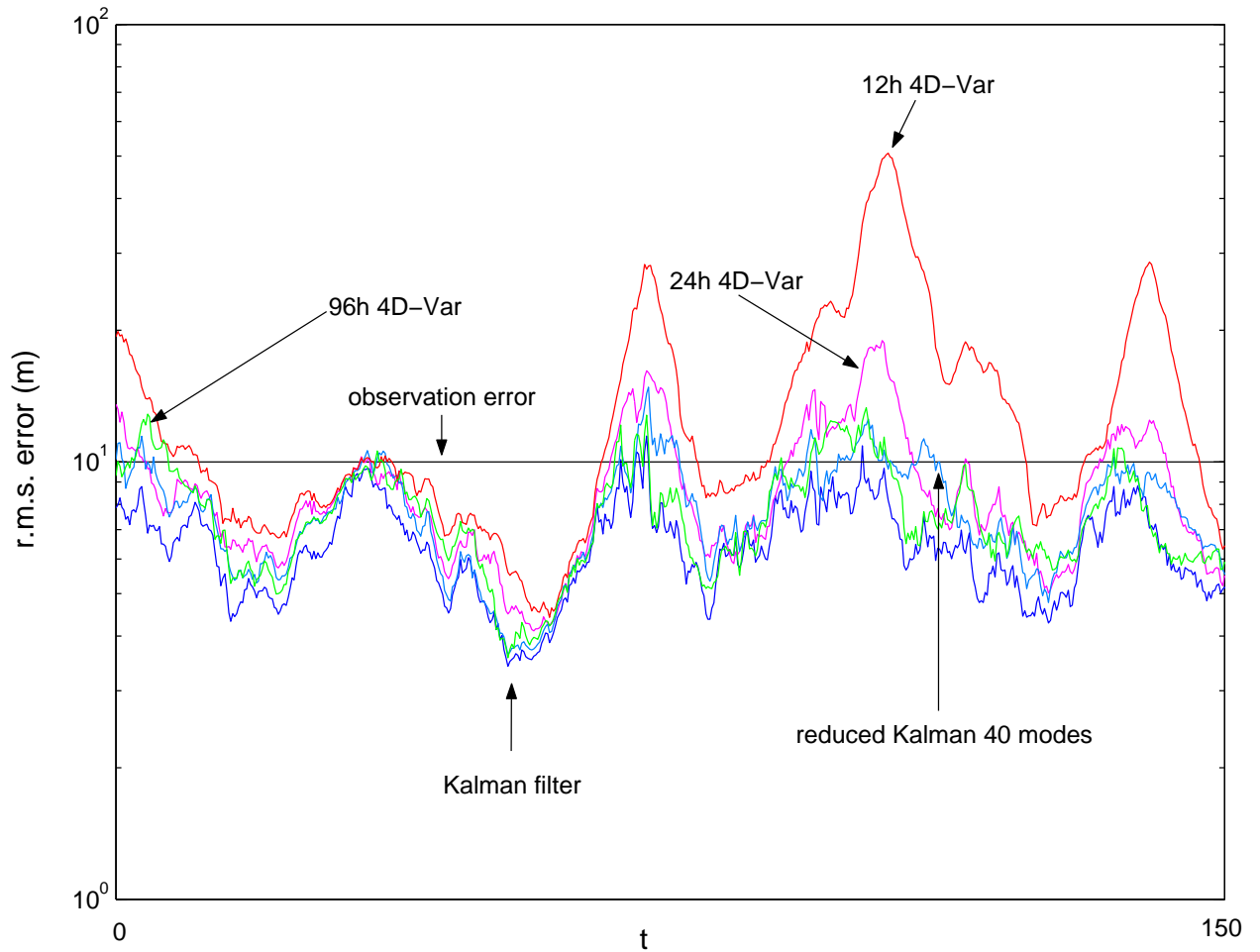


Figure 12: Error in the time dependent storm track model with model error. The data is assimilated with 4D-Var over the assimilation intervals of 12 *h*, 24 *h* and 96 *h*. The background \mathbf{B} is the identity. Also shown is the error obtained with sequential application of a Kalman filter and a reduced Kalman filter (resulting from a truncation to 40 dof out of the 400 dof of the system). The 4D-Var over 24 *h* performs nearly optimally. The far field loadings of the gain associated with the longer interval 4D-Var leads to a degradation of the performance of 4D-Var. 16 observations are assimilated with r.m.s. observational error of 10 *m*. The model error variance coefficient is $q = 12 \text{ m}^2 \text{ d}^{-1}$, so that a model error of 5 *m* accumulates in one day.

Approach of 4D-Var to Kalman filter as the number of observations increase With model error and 40 observations

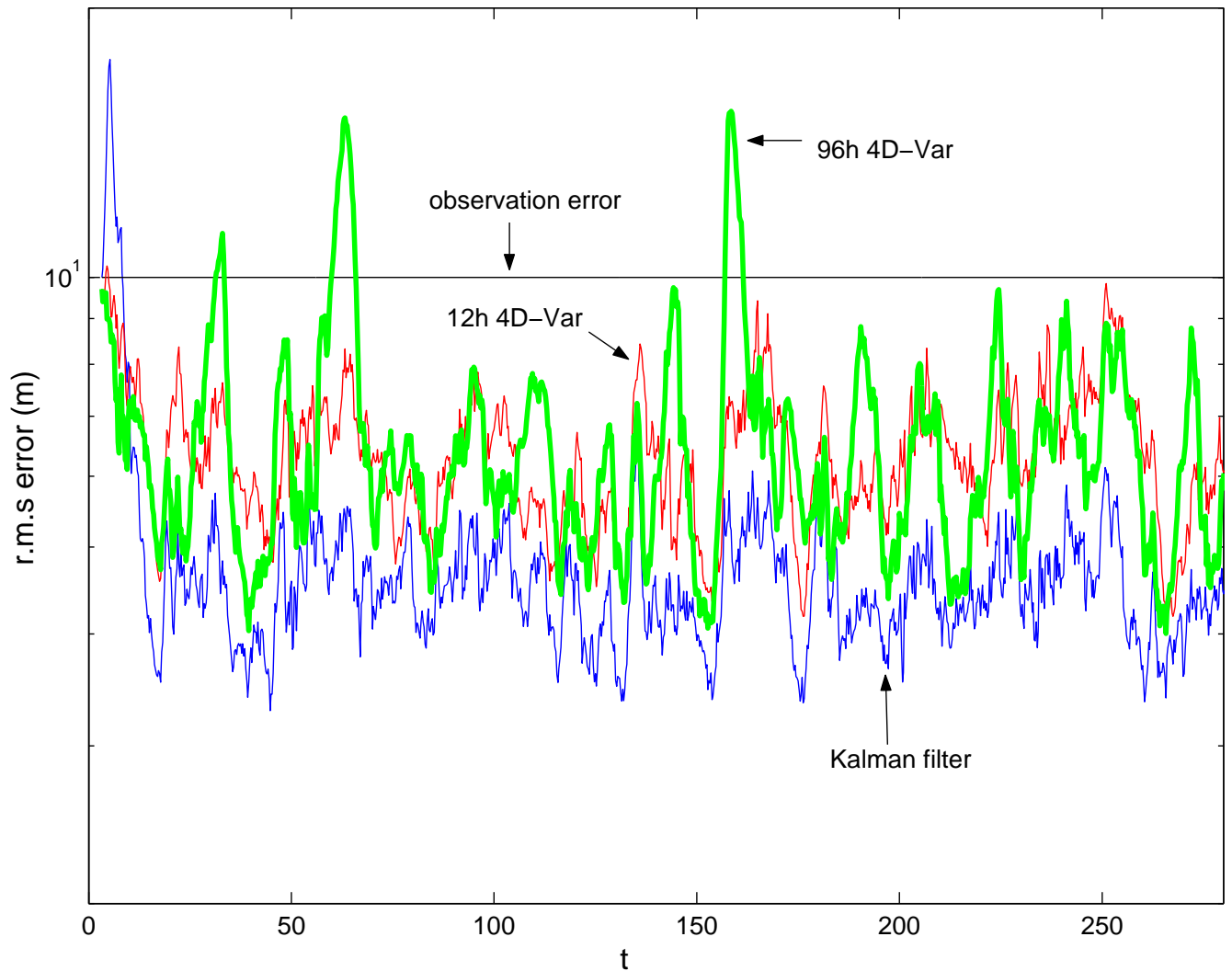


Figure 13: As in Fig. 12 but with 40 observations. The error has decreased with the assimilation of 40 observations. The assimilation intervals shown are 12 *h* and 96 *h*. The far field loadings of the 4D-Var gain leads to a degradation of the performance of 4D-Var over 96 *h*.

Error in 4D-Var as a function of the assimilation interval

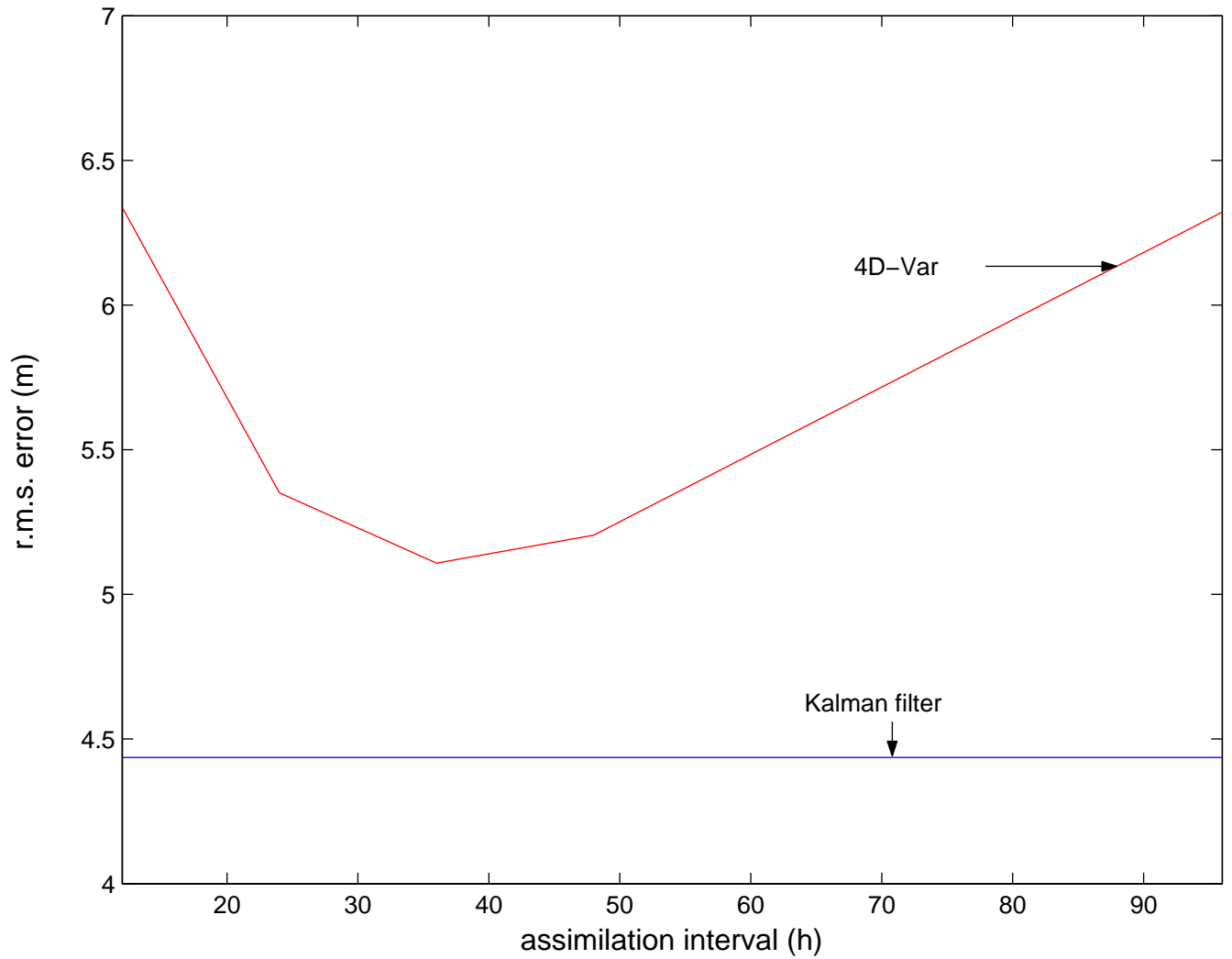


Figure 14: R.m.s. error in 4D-Var assimilations in the time dependent storm track model with model error as a function of assimilation interval. The best 4D-Var performance is achieved in this example for assimilation over the interval 36 h . Also shown is the error obtained with the Kalman filter. 40 observations are assimilated with r.m.s. observational error of 10 m ; the model error variance is $q = 12 \text{ m}^2 \text{ d}^{-1}$, so that a model error of 5 m accumulates in one day.

Snapshots of the gains of the Kalman filter with model error and of 4D-Var.

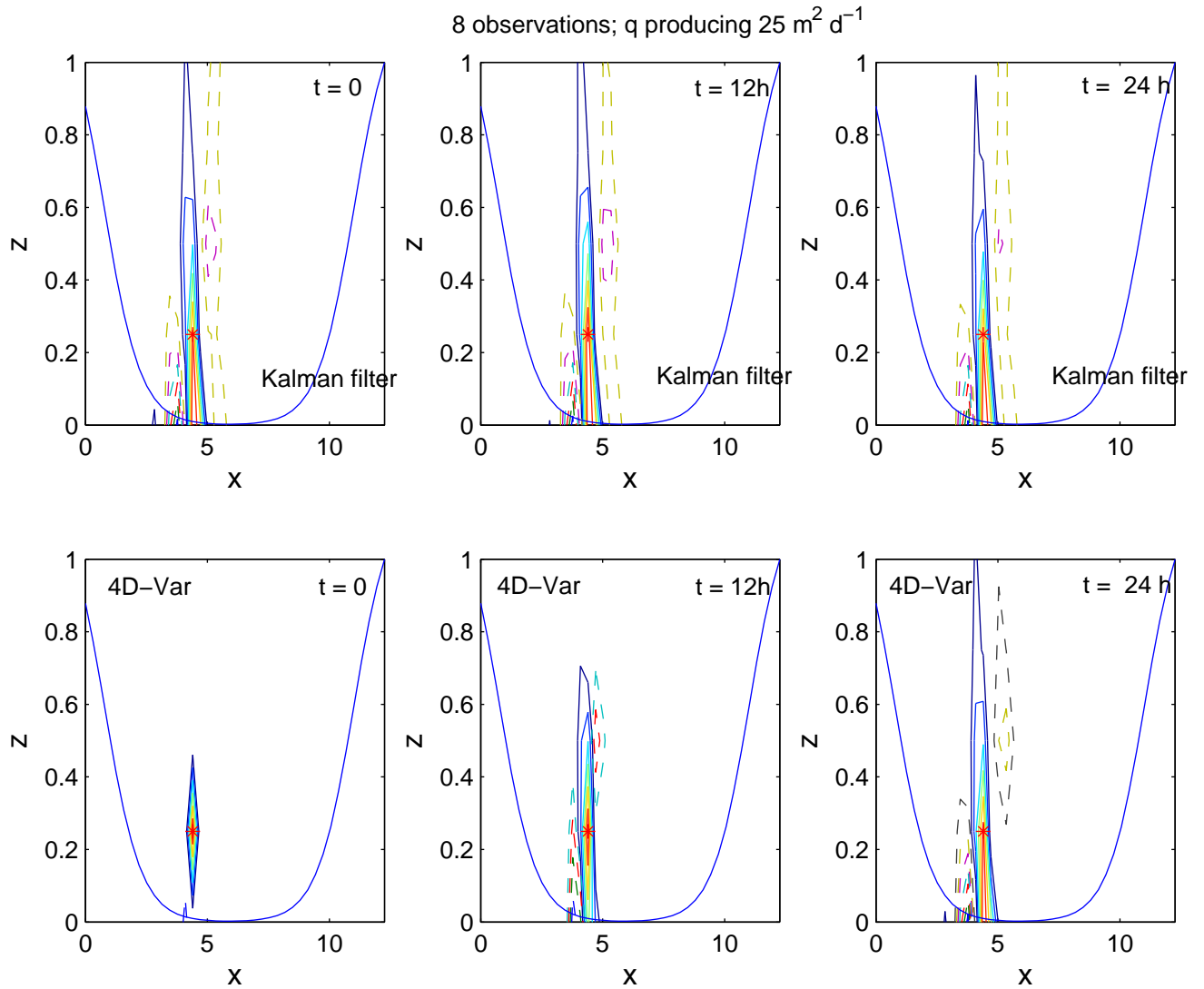


Figure 15: Top panels: gain of the Kalman filter in sequential assimilation of 8 observations in the time dependent storm track model with model error. Bottom panels: corresponding gains obtained from 4D-Var. The gains of the Kalman filter remain concentrated near the location of the observation. The corresponding gains obtained from 4D-Var are good over a 24 h assimilation interval. The model error variance coefficient is $q = 12 \text{ m}^2 \text{ d}^{-1}$, so that a model error of 5 m accumulates in one day.

Using the error covariance from the reduced Kalman filter with model error in 4D-Var makes the 12 h 4D-Var nearly optimal

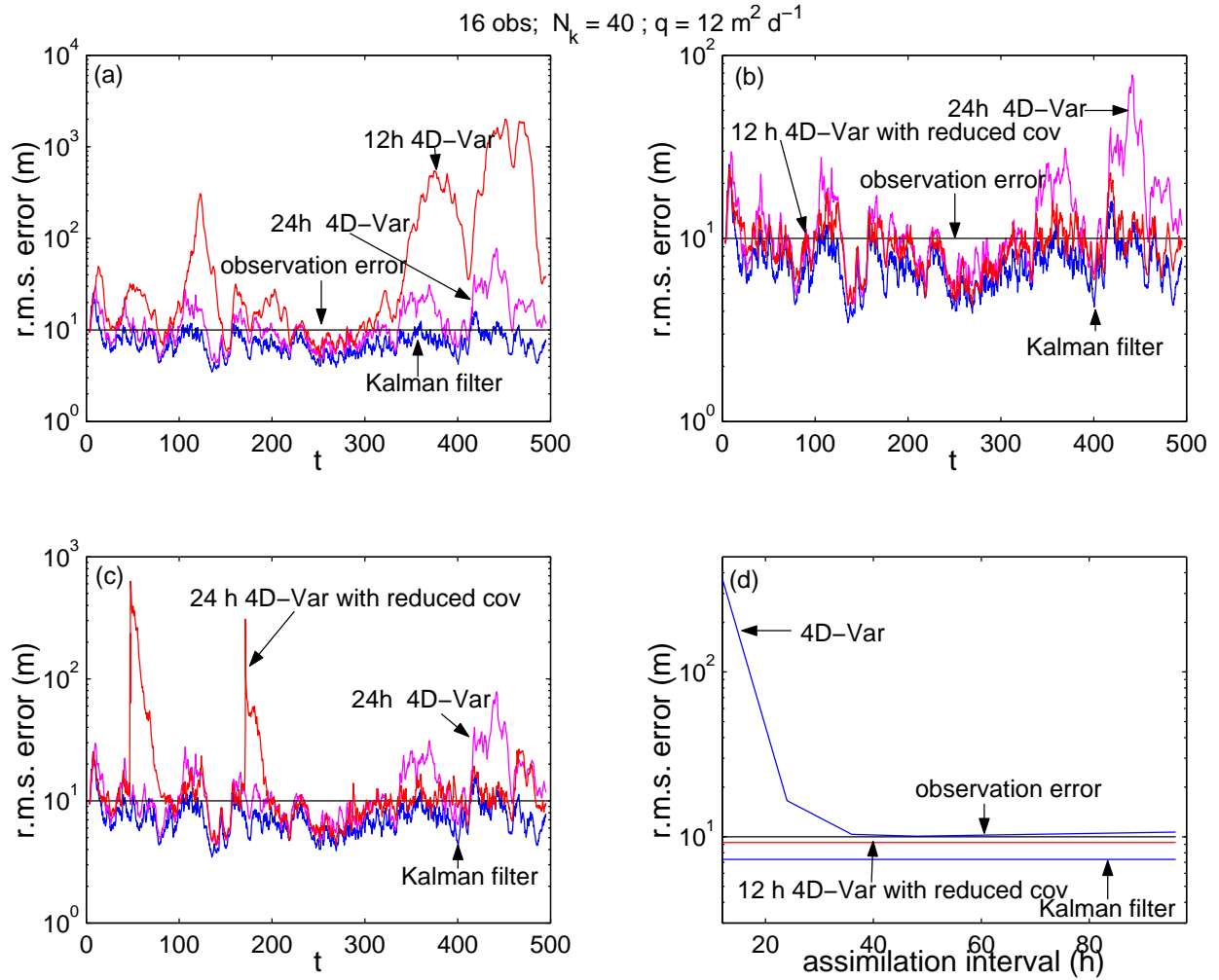


Figure 16: Error in a simulation of the time dependent storm track model with model error. Panel (a): comparison of the errors in a 12 h and 24 h 4D-Var with the error in the full Kalman filter. Panel (b): comparison of the error in a 24 h 4D-Var with the error in a 12 h 4D-Var in which the isotropic static \mathbf{B} has been preconditioned with the error covariance obtained from a reduced rank Kalman filter with balanced truncation. The reduced rank Kalman filter has been obtained with model error. In the truncated system 40 dof have been retained out of the 400 dof of the system. The isotropic \mathbf{B} introduced to the reduced rank covariance has amplitude equal to the smallest eigenvalue of the reduced rank covariance. Also shown is the error resulting from the Kalman filter. The 12 h 4D-Var performance is nearly optimal. Panel (c): comparison of the error in a 24 h 4D-Var with the error in a 24 h 4D-Var in which the isotropic static \mathbf{B} has been preconditioned with the error covariance obtained from the reduced Kalman filter. The 24 h 4D-Var preconditioned with the covariance from the reduced Kalman filter propagates the covariance without model error longer and its performance is worse than that of the corresponding 12 h 4D-Var. Panel (d): r.m.s. error in 4D-Var assimilations in the time dependent storm track model with model error as a function of assimilation interval. Also shown is the error obtained with sequential application of a Kalman filter and the error from the 12 h 4D-Var which was preconditioned with the reduced rank covariance. 16 observations are assimilated with r.m.s. observational error of 10 m. The model error variance coefficient is $q = 12 \text{ m}^2 \text{ d}^{-1}$, so that a model error of 5 m accumulates after a day.

Using the reduced error covariance from the reduced Kalman filter with no model error in 4D-Var degrades 4D-Var performance

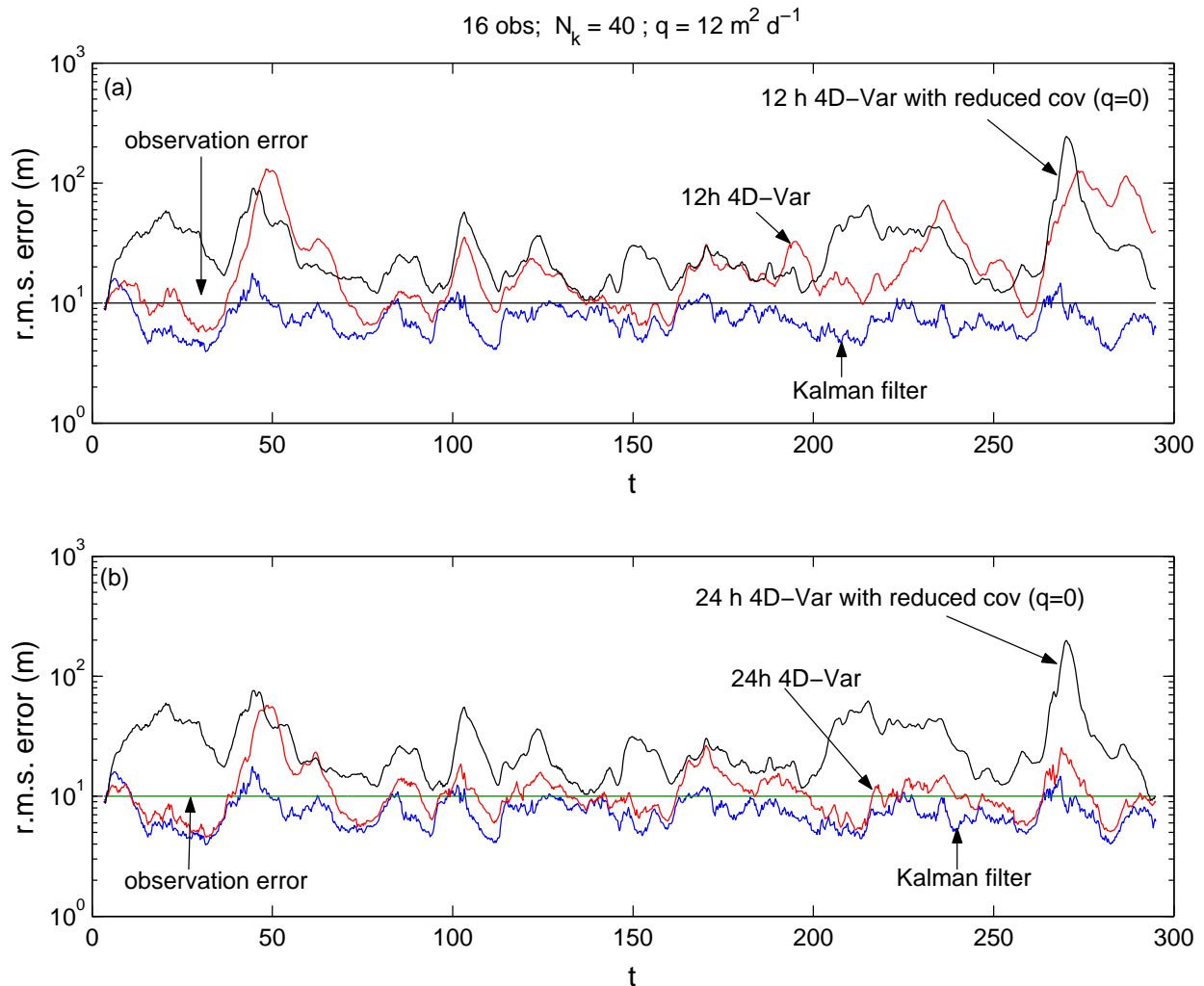


Figure 17: Error in a simulation of the time dependent storm track error model with model error. Panel (a): comparison of the error in a 12 h 4D-Var with the error in a 12 h 4D-Var in which the isotropic static \mathbf{B} has been preconditioned with the error covariance obtained from a reduced rank Kalman filter with balanced truncation. The reduced rank Kalman filter has been obtained with no model error. In the truncated system 40 dof have been retained out of the 400 dof of the system. The isotropic \mathbf{B} introduced to the reduced rank covariance has amplitude equal to the smallest eigenvalue of the reduced rank covariance. Also shown is the error resulting from the Kalman filter. The introduction of the covariance from the reduced model with no model error degrades the performance of the 4D-Var. Panel (b): comparison of the error in a 24 h 4D-Var with the error in a 24 h 4D-Var in which the isotropic static \mathbf{B} has been preconditioned with the error covariance obtained from the reduced rank Kalman filter with balanced truncation with no model error. Also shown is the error resulting from the Kalman filter. The introduction of the covariance from the reduced model with no model error degrades the performance of 4D-Var and makes this 24 h 4D-Var perform like the 12 h 4D-Var, indicating that the reduced rank covariance with its far field loadings dominates the gains in the 4D-Var. 16 observations are assimilated with r.m.s. observational error of 10 m. The model error variance coefficient is $q = 12 \text{ m}^2 \text{ d}^{-1}$, so that a model error of 5 m accumulates in one day.

Cross section of strm func 20030115 1200 step 48 Expver ef7z

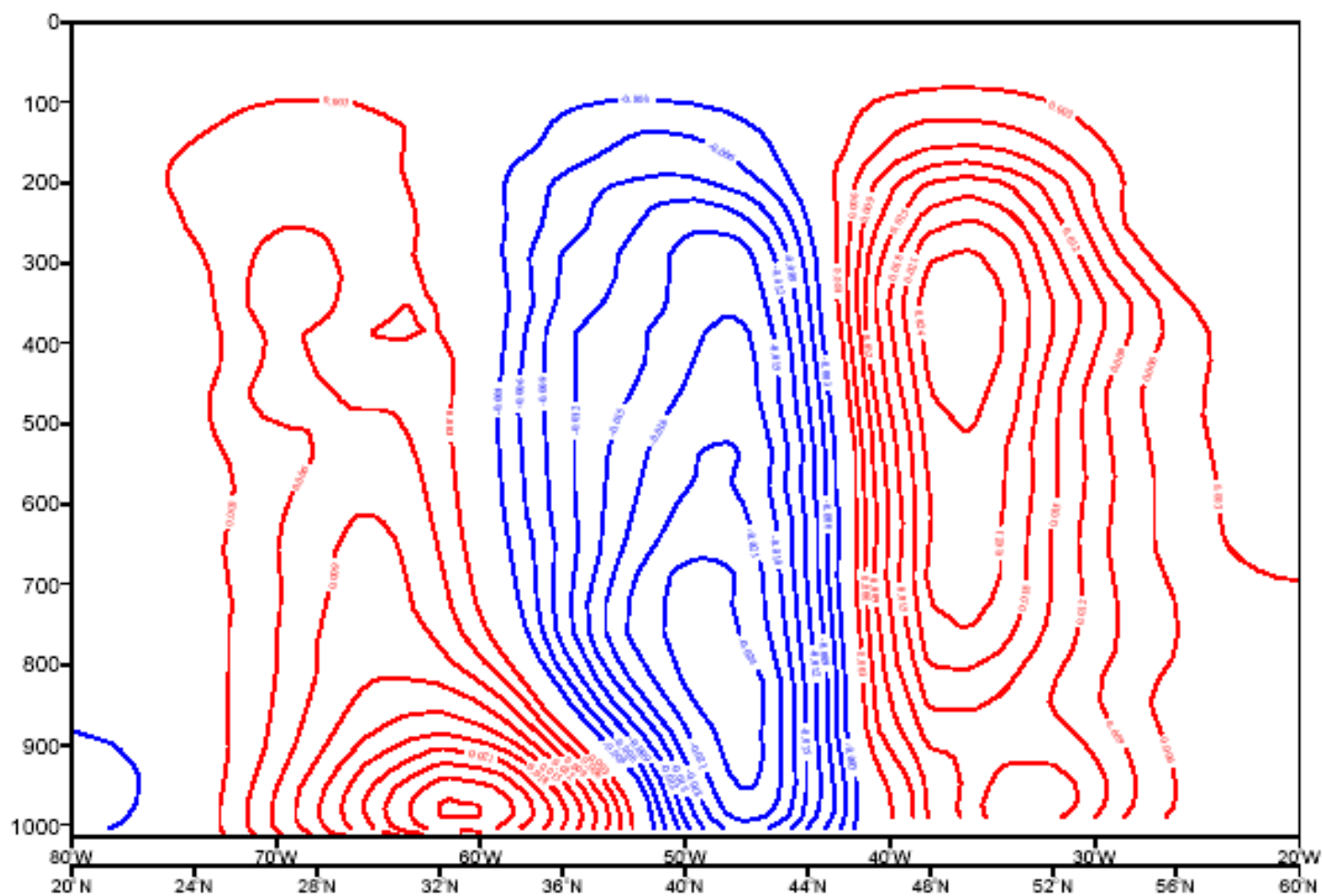


Figure 13: Cross section of the leading basis vector for 48h finite-horizon balancing.

Cross section of strm func 20030115 1200 step 48 Expver ef7z

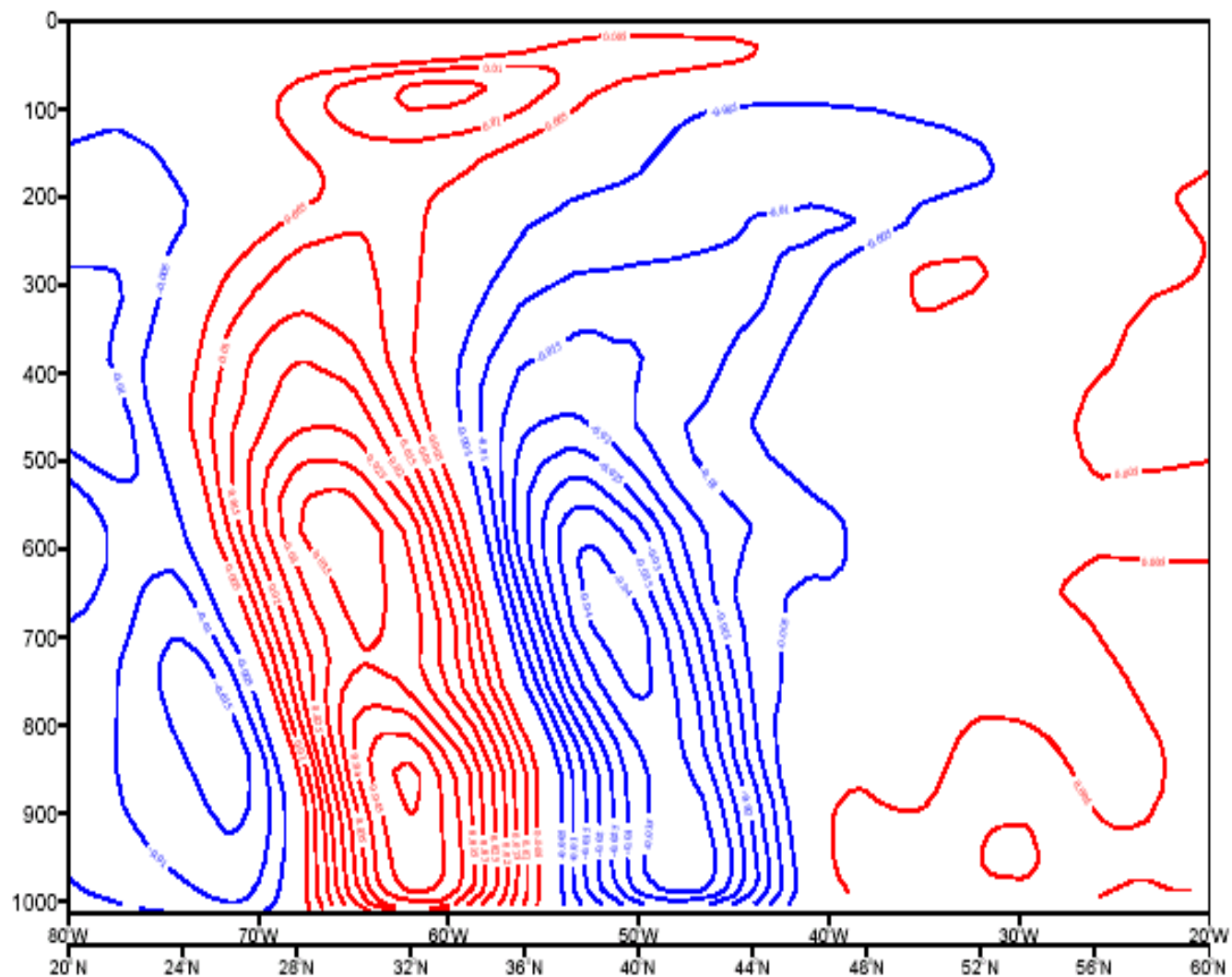


Figure 14: Cross section of the leading bi-orthogonal vector for 48h finite-horizon balancing.

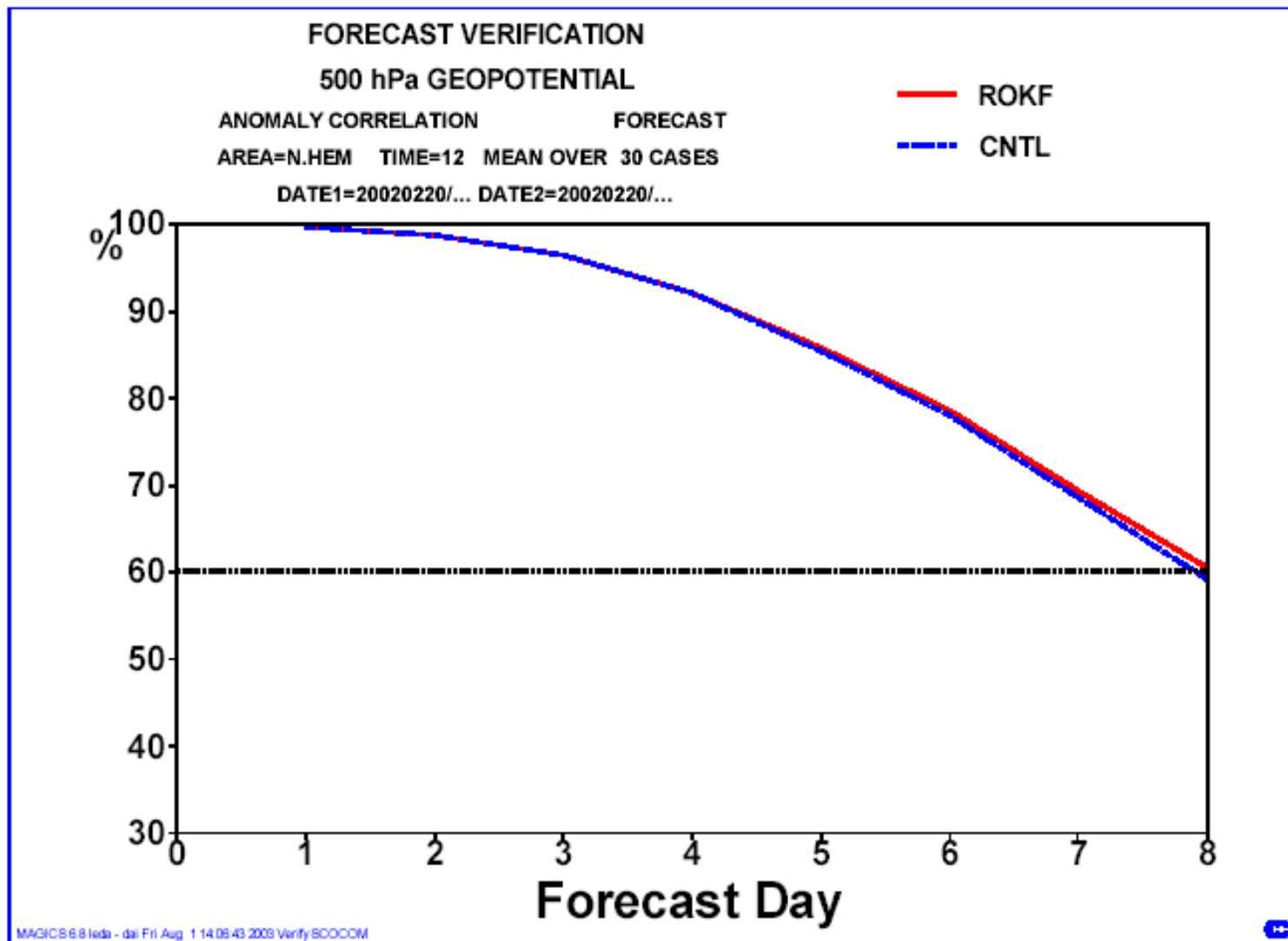


Figure 21: 500hPa geopotential anomaly correlation scores for the northern hemisphere for the ROKF using singular vector reduction with $T_{opt}=48h$

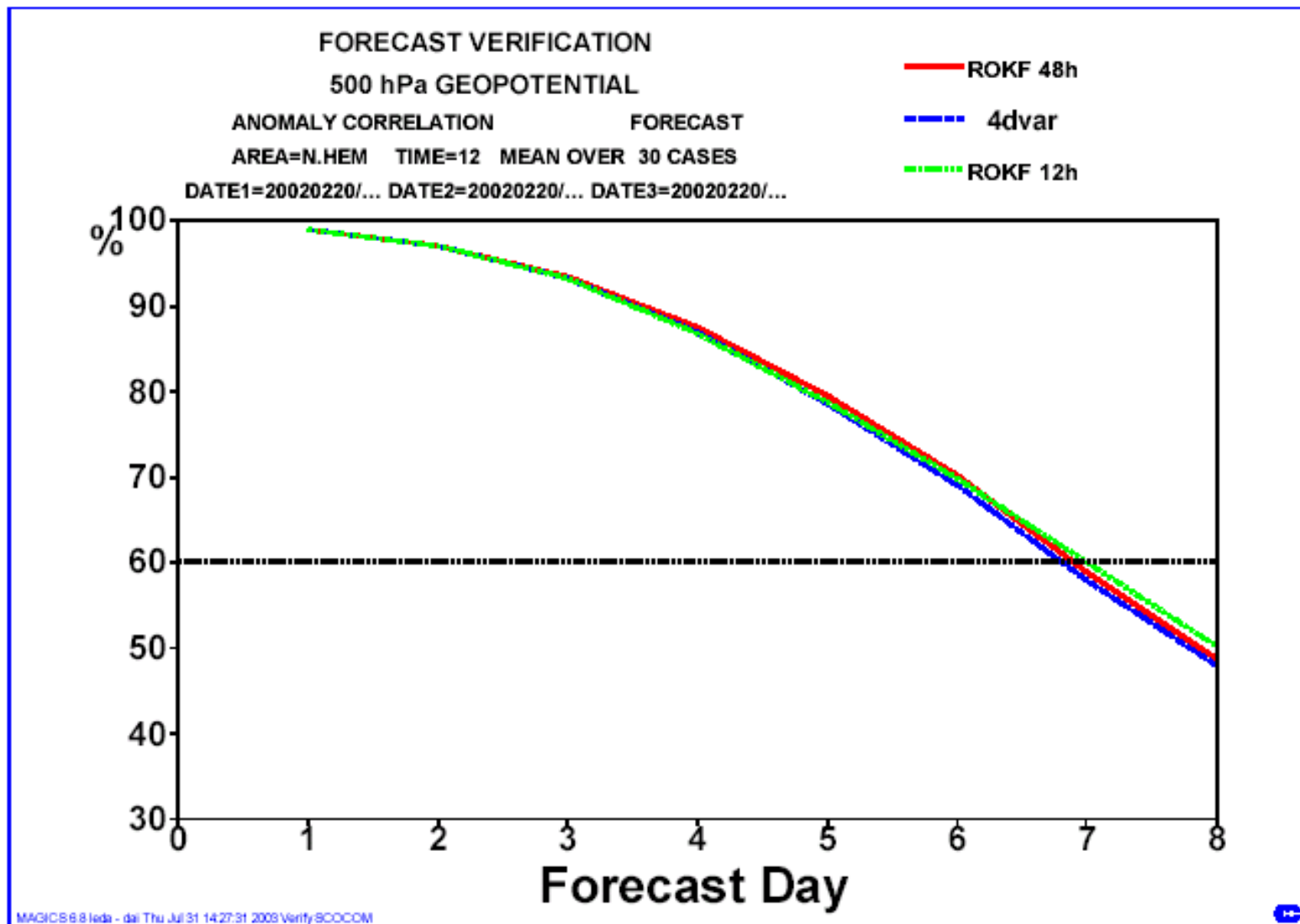


Figure 23: 500hPa geopotential anomaly correlation scores for the northern hemisphere for the ROKF using singular vector reduction with $T_{opt}=12h$ and $T_{opt}=48h$ using only conventional observations.

CONCLUSIONS

- Implementing optimal observer strategies requires that the state dependent error structure be accurately estimated. However, the high state dimension of the forecast system presents an obstacle to determining the state dependent error covariance.
- The dynamically relevant dimension of the forecast error system is far smaller than the state dimension and this fact can be exploited to obtain a reduced order forecast error system from which the state dependent error structure can be obtained.
- Assimilation systems can be usefully analyzed as Luenberger observers. The observer system is stable but with transient growth. The generalized stability analysis of the observer reveals the potential for analysis failures.
- In the presence of model error as the number of observations increases and redundancy in the observations is attained the r.m.s. analysis error in a Kalman filter assimilation decreases with observation number, n , as $n^{-1/4}$. In 4D-Var under similar conditions the analysis error asymptotes to a constant value.
- The gain in a perfect model has far field loadings. The presence of model error localizes the gains.
- Covariances from the reduced order system may be used to precondition the background B in 4D-Var. If model error is introduced in the propagation of the reduced rank covariance the 12 h 4D-Var performs nearly optimally. On the other hand when the reduced covariance is obtained with no model error the performance of the preconditioned 4D-Var is degraded.